Irreversible Activation of the Gonadotropin-Releasing Hormone Receptor by Photoaffinity Cross-Linking: Localization of Attachment Site to Cys Residue in N-Terminal Segment

James S. Davidson,*,‡ Daniel Assefa,‡ Adam Pawson,‡ Peter Davies,‡ Janet Hapgood,‡ Inga Becker,‡ Colleen Flanagan,§ Roger Roeske,|| and Robert Millar‡

M.R.C. Regulatory Peptides Research Unit, Department of Chemical Pathology, University of Cape Town Medical School, Observatory 7925, South Africa, Endocrine Laboratory, Department of Medicine, University of Cape Town Medical School, Observatory 7925, South Africa, and Department of Biochemistry and Molecular Biology, Indiana University School of Medicine, Indianapolis, Indiana 46202-5122

Received June 9, 1997; Revised Manuscript Received August 1, 1997[⊗]

ABSTRACT: Photoaffinity cross-linking with [azidobenzoyl-D-Lys[6]]GnRH leads to irreversible activation of the gonadotropin-releasing hormone (GnRH) receptor. In order to localize the cross-linking site, the disulfide bridge structure was initially probed by mutagenesis. A consistent pattern of changes in the ability of GnRH to stimulate signal transduction after Ser substitutions of extracellularly located Cys residues indicated that Cys14 in the N-terminal domain is connected to Cys200 in the second extracellular loop, while Cys196 in this loop is connected to the highly conserved Cys114 at the extracellular end of transmembrane helix 3. Protein chemical analysis of radioactive fragments of cross-linked GnRH receptor following deglycosylation and enzymatic digest with endoproteinase Glu-C and trypsin before and after introduction or elimination of potential protease cleavage sites indicated that ^{125}I[azidobenzoyl-D-Lys[6]]GnRH cross-links to a segment comprising residues 12−18 of the N-terminal domain. The existence of the Cys114−Cys196 bridge was directly confirmed as a labeled fragment, including that Cys114 was resolvable only under reducing conditions. The observation that the cross-linked N-terminal enzymatic fragments had identical apparent size under non-reducing conditions shows that the cross-linking reaction disconnected the disulfide bridge between Cys14 and Cys200 and indicates that Cys14 is probably the residue involved in cross-linking of the ligand. It is concluded that covalent tethering of GnRH through a photoreactive side chain located at position 6 in the middle of the peptide leads to continued activation of the receptor presumably through covalent binding to Cys14 in the N-terminal domain of the receptor.

The hypothalamic decapeptide gonadotropin-releasing hormone (GnRH) is the central regulator of the reproductive system, acting via receptors on pituitary gonadotrope cells. GnRH receptors (GnRHRs) from mouse, rat, human, sheep, and cow are members of the G-protein coupled receptor (GPCR) superfamily (*1*−*7*) and are coupled via $G_{q/11}$ to activation of phospholipase C, leading to calcium signalling (*8*−*10*) and the release of gonadotropins by regulated exocytosis (*11*−*13*).

Knowledge of the disulfide bridge structure is a prerequisite for the construction of molecular models of the GnRHR, which include the extracellular domains. The pituitary GnRHR from human, mouse, rat, sheep, and cow has four cysteine residues in its extracellular domains (Figure 1). A Cys residue at the position of C114, at the C-terminal end of extracellular loop 1, is highly conserved throughout the GPCR superfamily, not only in the main rhodopsin-like group but also in the metabotropic glutamate receptor group and the parathyroid hormone receptor group of receptors (*14*−*16*), making this motif the most widely conserved in the superfamily. It has been suggested that the non-conserved Cys (C14) in the mammalian GnRHR may form a second disulfide bridge, as shown in Figure 1, linking the N-terminus with the second intracellular loop (*1*).

In this study, we have utilized a strategy of photoaffinity labeling and enzymatic cleavage of the receptor combined with naturally occurring as well as engineered mutations of the protease cleavage sites to localize the attachment site of a photoaffinity ligand. The results indicate that ^{125}I[azidobenzoyl-D-Lys[6]]GnRH attaches to a 7-residue segment of the N-terminal domain. Comparison of the sizes of labeled fragments under reducing and non-reducing conditions confirms directly the existence of a disulfide bridge between C114 and the second extracellular loop. Mutational analysis indicates that the other two cysteines, C14 and C200, form a second disulfide bridge linking the N-terminal domain to the second extracellular loop.

EXPERIMENTAL PROCEDURES

Site-Directed Mutagenesis. The construction of mutations (Asp to Asn and Glu to Gln) at all extracellular and transmembrane acidic residues of the mouse GnRHR has been previously described (*17*). The human GnRHR cDNA (*5*) was shortened by removal of 1.3 kb of the 3′ untranslated region and cloned into the *Eco*RV site of the phagemid pcDNA1/Amp (InVitrogen). Oligonucleotide-directed mu-

* Corresponding author fax: +27-21-448-8150, phone: +27-21-406-6354, e-mail: JAMES@CHEMPATH.UCT.AC.ZA.

‡ Department of Chemical Pathology, University of Cape Town Medical School.

§ Department of Medicine, University of Cape Town Medical School.

|| Department of Biochemistry and Molecular Biology, Indiana University School of Medicine.

⊗ Abstract published in *Advance ACS Abstracts,* October 1, 1997.

S0006-2960(97)01377-9 CCC: $14.00

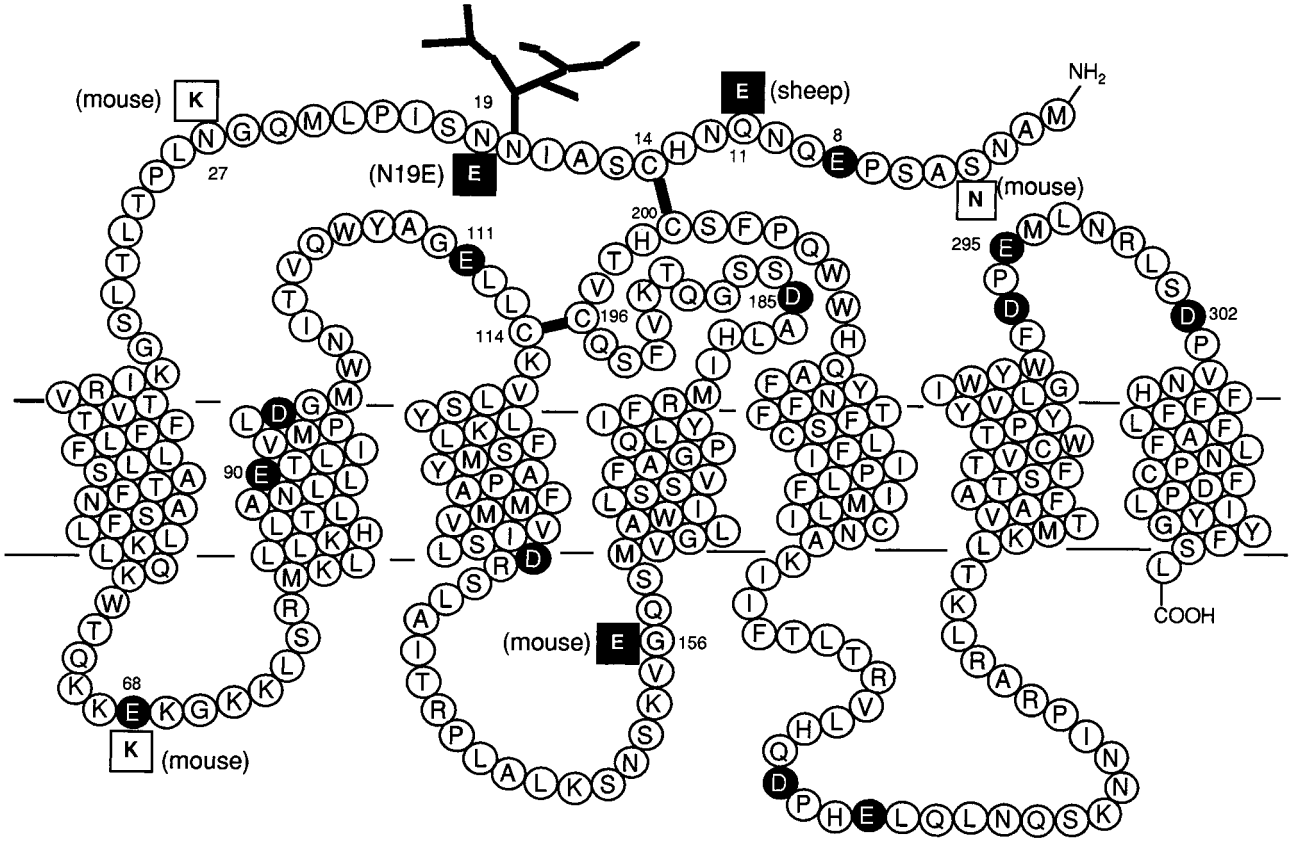

FIGURE 1: Amino acid sequence of the human GnRH receptor (circled residues). Sequence differences in the mouse, sheep, and mutant receptors that resulted in additional protease cleavage sites are shown in squares. Potential Glu-C cleavage sites are shown as filled circles. Residues referred to in the text are numbered.

tagenesis was performed using the method of Kunkel et al. (18). After being passed through *Escherichia coli* dut$^-$ung$^-$F′ strain CJ236, a uridine-containing single-stranded DNA template was prepared using VCS M13 helper phage (Stratagene). Mutant oligonucleotides were designed to encode the described amino acid substitutions as well as a silent restriction site, whenever possible. Oligonucleotides were phosphorylated with T4 polynucleotide kinase (Promega) and hybridized with the template, and second strand synthesis was completed using T7 DNA polymerase (Biorad) and T4 ligase (Biorad). Products of the reaction were used to transform competent *E. coli* strain XLI-blue. Plasmid DNA from ampicillin-resistant colonies was digested with the appropriate restriction enzyme and clones showing the additional restriction site were sequenced, confirming the mutations. Mutations are designated as in the following example: mE8Q refers to mouse GnRH receptor with Glu^8 mutated to Gln.

Transfection. Plasmid DNA for transfection was prepared using Qiagen columns (Qiagen) according to the manufacturer's instructions. COS-1 cells were cultured in DMEM (Gibco) containing 10% fetal calf serum in a 10% CO_2 atmosphere. The 3×10^6 cells were seeded into 100 mm diameter dishes and transfected 1 day later by a modification of the DEAE−dextran method (*19*). Cells were washed twice with phosphate-buffered saline, pH 7.4 (PBS), and then incubated with 4 mL/dish of serum-free DMEM containing 3.5−5 μg/mL of plasmid DNA and 0.3 mg/mL of DEAE−dextran for 4 h at 37 °C. This was replaced with DMEM containing 2% fetal calf serum and 150 μM chloroquine, and incubation was continued for 1 h at 37 °C. The cells were washed with PBS and finally cultured in DMEM with 10% fetal calf serum for 48 h before photoaffinity labeling or inositol phosphate assays.

Photoaffinity Labeling. [D-Lys^6]GnRH was synthesized by the solid phase method using Boc for α-amino protection and benzyl-based protecting groups for side chain functional groups and assembled on a Boc Arg (MTS) Pam resin using an Applied Biosystems Model 431A automated synthesizer, with couplings mediated by DCC/HOBt. [D-Lys^6-*N*-azidobenzoyl]GnRH was synthesized according to Hazum (*20*), by reacting [D-Lys^6]GnRH with azidobenzoyl *N*-hydroxysuccinimide ester (Sigma) in methanol for 4 h at room temperature. The reaction product was precipitated with 10 vol of diethyl ether, washed three times with ethyl acetate, dried under N_2, and dissolved in 50% methanol−water. The derivatized peptide was pure when visualized by iodine vapor staining after thin-layer chromatography on silica gel. It showed an absorbance peak at 271 nm, different from that of azidobenzoyl N-hydroxysuccinimide ester (285 nM). The absorbance at 271 nm was decreased by 70% after exposure to UV light. Five micrograms of the peptide was iodinated using chloramine T and purified on a reverse-phase C18 HPLC column, eluting as a single radioactive peak with a 0−60% acetonitrile gradient. All the above procedures were performed under minimal lighting. Iodinated ligand was stored at −70 °C. αT3 gonadotrope cells (*21*) or COS-1 cells transfected 48 h previously in 100 mm dishes were incubated with 1.2 mL of buffer A per dish, containing 5×10^6 cpm ^{125}I[D-Lys^6-*N*-azidobenzoyl]GnRH (approximately 4 nM) in the presence or absence of 2 μM unlabeled GnRH agonist, at 20 °C for 30 min in the dark. Buffer A consisted of 140 mM NaCl, 4 mM KCl, 20 mM HEPES, pH 7.4, 8 mM D-glucose, 0.5 mM $CaCl_2$, and 0.5 mM $MgCl_2$. The

dishes were irradiated for 60 s at a distance of 2 cm from a Spectroline TR-312A UV transilluminator and then washed with buffer A. The cells were detached in ice-cold binding buffer (10 mM Hepes, 1 mM EDTA, pH 7.4), homogenized with 15 strokes of a glass Dounce homogenizer, and centrifuged for 10 min at 400*g* to remove nuclei. The supernatant was centrifuged at 10000*g* for 30 min at 4 °C, and the membrane pellet was resuspended using a fine needle in 0.25 mL of binding buffer per dish of cells.

Enzymatic Cleavage. Labeled receptor samples were denatured by adding SDS to 0.5% and heating for 15 min at 60 °C and then diluted with binding buffer to decrease the SDS concentration to 0.2%, and Triton X-100 was added to a final concentration of 1%. Samples were deglycosylated with 3 U/mL of peptide N-glycosidase F (Boehringer Mannheim) at 37 °C for 18 h. Cleavage was performed with 100 μg/mL of endoproteinase Glu-C (Boehringer-Mannheim) for 18 h at 37 °C. Digested samples were mixed with SDS sample buffer, with or without 5% (v/v) 2-mercaptoethanol, and electrophoresed for 18 h at room temperature on three-phase SDS−polyacrylamide gels (4%, 10%, and 16.5% acrylamide) using a tricine buffer system as described for separation of peptides (*22*). The gels were fixed, stained with Coomassie Blue, dried, and autoradiographed.

Radioligand Binding. αT3 cells were homogenized in binding buffer and centrifuged at 15000*g* for 30 min at 4 °C. The membrane pellet was resuspended in binding buffer and incubated (7.5×10^5 cell equivalents/tube) with 60 000 cpm ^{125}I[D-Ala^6,N-Me-Leu^7,des-Gly^{10}-NHEt]GnRH and varying concentrations of dithiothreitol (DTT), *N*-ethylmaleimide (NEM), or iodoacetamide for 90 min on ice. The incubation was terminated by the addition of 3 mL of PBS containing 0.1% BSA and immediate filtration through GF/C filters (Whatman). Non-specific binding was estimated in the presence of 10^{-7}M unlabeled [D-Ala^6,N-Me-Leu^7,des-Gly^{10}-NHEt]GnRH.

Inositol Phosphate Production. Twenty-four hours after transfection, cells were labeled overnight with 2 μCi/mL of myo[2-^{3}H]inositol (Amersham) in 0.25 mL/well Medium 199 (Gibco) containing 5% fetal calf serum, washed twice in buffer A, and then stimulated with GnRH as indicated. Incubations were stopped with perchloric acid/phytic acid (PCA) solution, and following neutralization with KOH, total inositol phosphates were chromatographed on Dowex columns as previously described (*23*).

Data Reduction. Peptide concentrations required to stimulate half-maximal IP production (EC_{50}) were estimated by nonlinear regression to the equation $IP = IP_{max}/(1 + EC_{50}/A)$, where IP is the inositol phosphate response to concentration *A* of agonist, and IP_{max} is the maximal response, using Prism (Graphpad) software. Figures show representative experiments in which data points are the mean ± range of duplicate determinations.

RESULTS

Cross-Linking of [Azidobenzoyl-D-Lys^6]GnRH Causes Irreversible Activation of the GnRH Receptor. To determine the functional effect of covalently attaching the photoreactive GnRH agonist analog [azidobenzoyl-D-Lys^6]GnRH to the GnRH receptor, αT3 cells, a pituitary cell line expressing mouse GnRHRs, were prelabeled with [^{3}H]-inositol and then incubated with the peptide in the absence of Li^+. In the absence of UV irradiation, the peptide was efficiently washed off, as shown by the low level of inositol phosphate production during subsequent incubation in the presence of Li^+ (Table 1). However, when the cells were UV irradiated prior to washing, inositol phosphate production continued at a rate equal to that observed with maximal GnRH stimulation (Table 1). This indicates that, following covalent attachment of the agonist, the receptor is held in a permanently activated conformation.

Table 1: Cross-Linking of Photoreactive Agonist [Azidobenzoyl-D-Lys^6]GnRH Induces Irreversible GnRH Receptor Activation[a]

	inositol phosphates, cpm × 1000	
	−UV	+UV
[azidobenzoyl-D-Lys^6]GnRH, then wash	3.05 ± 0.30	48.7 ± 1.2
control: basal	1.25 ± 0.30	2.05 ± 0.30
control: GnRH, no wash	45.1 ± 3.4	40.7 ± 1.6

[a] αT3 cells prelabeled with [^{3}H]inositol were incubated with 10 nM [azidobenzoyl-D-Lys^6]GnRH in dim light in the absence of Li^+ for 10 min, then exposed to UV irradiation where indicated, followed by three washes, and finally incubated in buffer containing 10 mM Li^+ for 15 min. Control cells were incubated in the absence (basal) or presence (GnRH) of 100 nM GnRH for 15 min in the presence of Li^+.

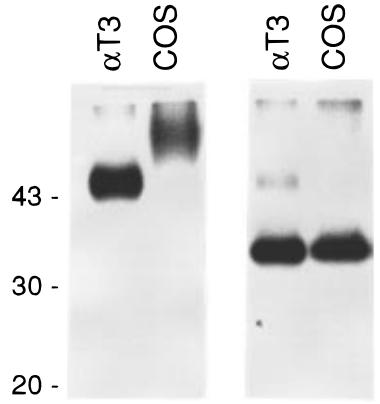

FIGURE 2: SDS−PAGE autoradiograph of photoaffinity labeled GnRH receptors. Intact αT3 mouse pituitary cells (αT3) and COS-1 cells expressing mouse wild-type GnRHR (COS) were photoaffinity labeled and prepared without deglycosylation (left panel) and with deglycosylation (right panel) as described under Experimental Procedures.

Localization of the Cross-Link Site of ^{125}I[D-Lys^6-N-Azidobenzoyl]GnRH. After being photoaffinity labeled with ^{125}I[D-Lys^6-N-azidobenzoyl]GnRH, membranes expressing GnRHRs showed broad-labeled bands of apparent molecular weight (MW_{app}) 60−75 kDa in COS-1 cells and 43−50 kDa in αT3 cells (Figure 2), as previously described (*20*, *24*−*26*). These bands represented GnRHRs since (a) labeling was abolished in the presence of 10^{-6} M unlabeled GnRH agonist and (b) no such labeled bands were present in untransfected cells (*26*). After deglycosylation, the receptors from both cell types migrated as sharp bands of identical mobility with MW_{app} 32 kDa (Figure 2), indicating that the broadness of the bands is due to heterogeneity of glycosylation. It was evident that GnRHRs expressed in COS-1 cells are glycosylated to a greater extent than those expressed endogenously in the gonadotrope-derived αT3 pituitary tumor cell line. The result of deglycosylation also shows that the photoreactive peptide cross-links to the protein rather than the carbohydrate moiety.

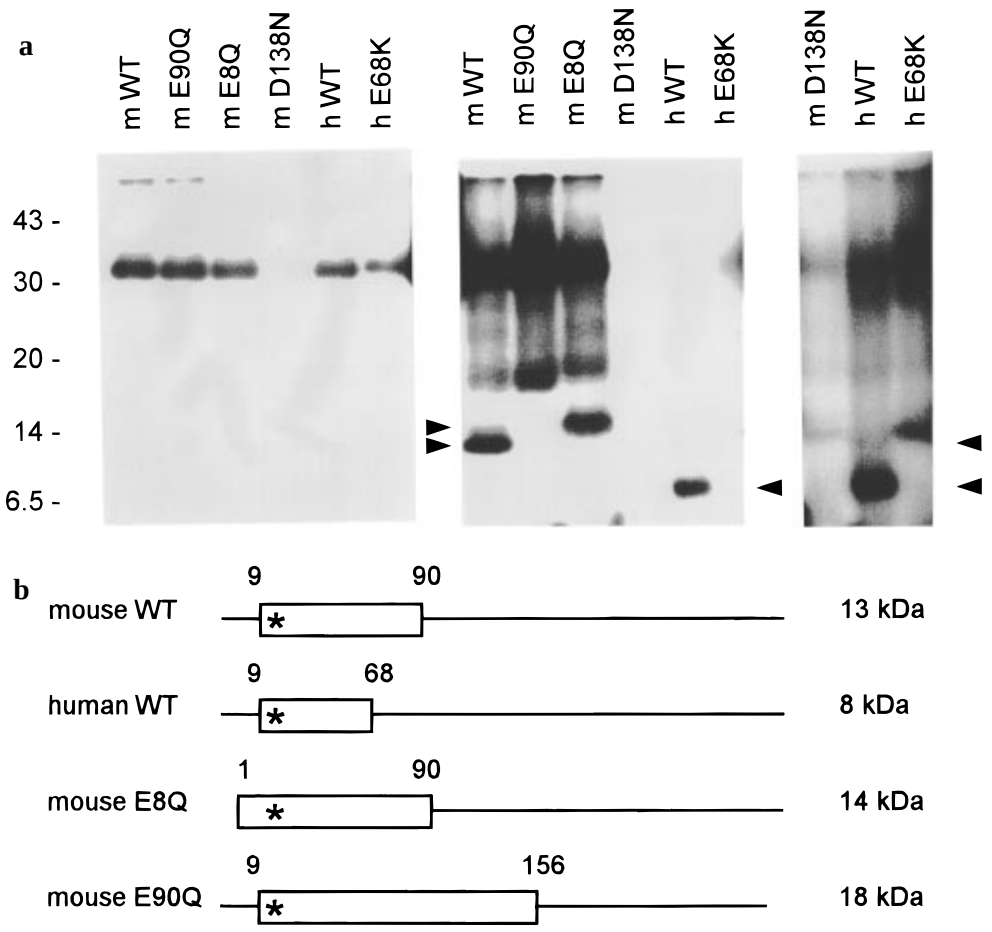

FIGURE 3: Endoproteinase Glu-C cleavage of photoaffinity labeled wild-type and mutant GnRH receptors (reducing conditions). (a) COS-1 cells expressing mouse or human GnRHRs were photoaffinity labeled; membrane suspensions were solubilized, deglycosylated, and digested with Glu-C under nonreducing conditions as described under Experimental Procedures. Following digestion, β-mercaptoethanol was added to a final concentration of 2% (v/v) prior to gel electrophoresis and autoradiography. Left panel: Deglycosylation only. Middle panel: Deglycosylation followed by Glu-C digestion. Right panel: Same gel as middle panel, with rightmost three lanes exposed for optimal visibility of 13 kDa bands in mouse D138N and human WT receptors. Arrowheads indicate 8, 13, and 14 kDa labeled fragments referred to in the text. (b) Location and expected sizes of Glu-C fragments. The box indicates the labeled fragment, while the asterisk (*) indicates the attachment site of the radiolabeled peptide.

Photoaffinity labeled GnRHRs were deglycosylated and then digested with endoproteinase Glu-C, which cleaves at the carboxy-terminal side of glutamic acid residues and at aspartic acid residues under certain conditions (*27*). Potential Glu-C cleavage sites are shown in Figure 1. Mouse wild-type (mWT) receptors yielded a labeled fragment of MW_{app} 13 kDa (Figure 3, middle panel, mWT). In contrast, mutant mE8Q (mouse receptor, Glu^8 to Gln^8 mutation) yielded a slightly larger fragment of MW_{app} 14 kDa (Figure 3, middle panel, mE8Q). This indicates that the fragment containing the attachment site is bounded by residue E8 on its N-terminal side. In place of the 13 kDA fragment, the mutant mE90Q showed a larger fragment of MW_{app} 18 kDa under reducing conditions (Figure 3, middle panel, mE90Q), which indicates that the fragment seen in the mWT receptor is bounded by E90 on its C-terminal side. Receptors mutated at potential Glu-C cleavage sites mD138N (Figure 3, right panel), mE111Q, mD185N, and mE294Q (not shown) showed the same 13 kDa fragment as the mWT receptor, confirming that the labeled fragment is not bounded by any of these residues.

The human wild-type (hWT) GnRHR contains a potential Glu-C cleavage site at E68 in the first intracellular loop that is not present in the mouse receptor (Figure 1). After Glu-C digestion, the hWT receptor yielded a band of MW_{app} 8 kDa (Figure 3, middle and right panels, hWT). In contrast, in the mutant hE68K, this was replaced by a MW_{app} 13 kDa band of identical mobility to that seen in the mWT receptor (Figure 3, right panel). This indicates that Glu-C cleaves at E68 and localizes the attachment site of the photoaffinity ligand to between residues 9 and 68 of the human receptor.

The attachment site was localized further by constructing a mutant receptor hN19E with an additional Glu-C site at position 19 and by making use of the sheep GnRHR, which has a Glu-C site at E11 (*6*). Glu-C digestion of the sheep receptor yielded labeled doublet bands of $\pm$8 kDa due to partial cleavage (Figure 4). The smaller fragment of the doublet was slightly smaller than in the hWT receptor, as expected for cleavage at E11, indicating the attachment site is C-terminal to residue 11. The hN19E receptor was labeled efficiently by the photoreactive peptide, and Glu-C cleaved this mutant receptor efficiently as shown by disappearance of the intact deglycosylated MW_{app} 32 kDa species (Figure 4). However, the hN19E receptor yielded no visible labeled fragment, indicating that the labeled fragment must have been smaller than MW_{app} 3 kDa and was not resolved from the residual free-labeled peptide migrating with MW_{app} less than 3 kDa. This places the attachment site N-terminal to residue 19, since if it were on the C-terminal side of residue 19 the labeled fragment would comprise 59 residues including the

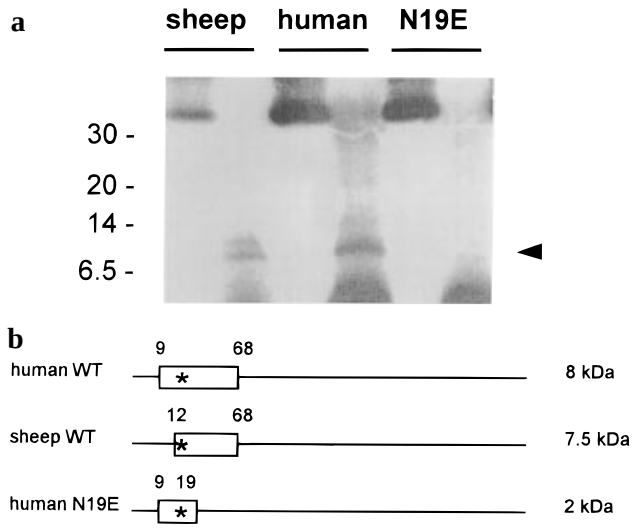

FIGURE 4: Endoproteinase Glu-C cleavage of photoaffinity labeled wild-type and mutant GnRH receptors (reducing conditions). (a) COS-1 cells expressing human or sheep GnRHRs were photoaffinity labeled; membrane suspensions were solubilized, deglycosylated, and digested with Glu-C under nonreducing conditions as described under Experimental Procedures. Following digestion, β-mercaptoethanol was added to a final concentration of 2% (v/v) prior to gel electrophoresis and autoradiography. In each pair of lanes, the left-hand lane shows the receptor after deglycosylation only, and the right-hand lane shows the receptor after deglycosylation and Glu-C cleavage. Arrowhead indicates 8 kDa fragments referred to in the text. (b) Location and expected sizes of Glu-C fragments. The box indicates the labeled fragment, while the asterisk (*) indicates the attachment site of the radiolabeled peptide.

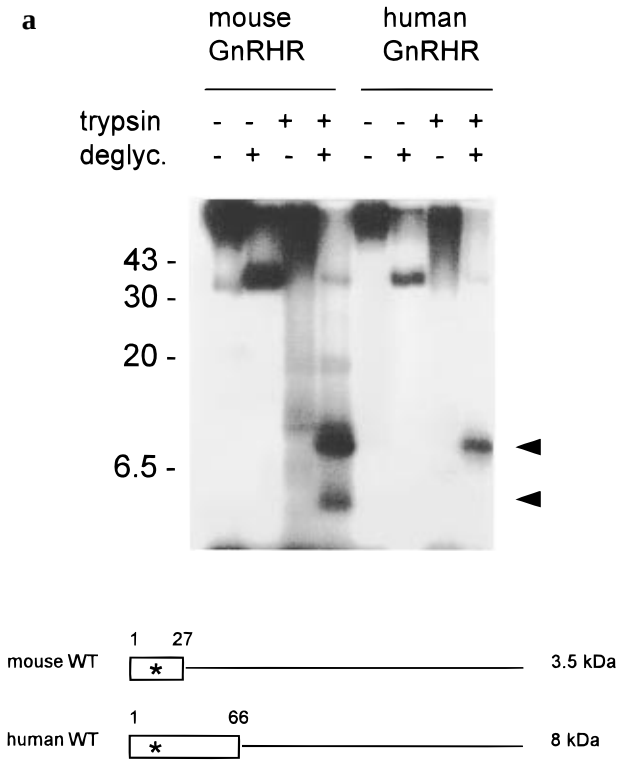

FIGURE 5: Trypsin cleavage generates a labeled 3.5 kDa fragment from mouse but not human photoaffinity labeled GnRHRs. (a) Intact COS-1 cells expressing mouse or human wild-type GnRHRs were photoaffinity labeled, and membrane suspensions were prepared as described under *Experimental Procedures*. Membrane suspensions were digested with trypsin (100 μg/mL at 37 °C for 18 h), followed by heat inactivation (60 °C for 30 min), addition of 50 μg/mL TLCK and 100 μg/mL soybean trypsin inhibitor, and then deglycosylated with 10 U/mL peptide N-glycosidase F at 37 °C for 6 h where indicated. Gel electrophoresis was performed under reducing conditions, followed by autoradiography. Arrowheads indicate the 3.5 and 8 kDa fragments referred to in the text. (b) Location and expected sizes of tryptic fragments. The box indicates the labeled fragment, while the asterisk (*) indicates the attachment site of the radiolabeled peptide.

decapeptide ligand, with an expected MW_{app} of 7 kDa, and would therefore have been easily resolved. Residue 19 can be excluded as the attachment site since modification of the glutamic acid side chain by a covalently linked peptide would be expected to abolish cleavage by Glu-C at that site.

Localization of the cross-link site to the N-terminal domain of the receptor was confirmed independently utilizing trypsin cleavage. The mouse GnRHR has a potential tryptic cleavage site at K27, which is absent in the human receptor (Figure 1). Trypsin digestion was performed in the absence of detergent to minimize cleavage at the juxta-membrane basic residues at the extracellular end of transmembrane helix 1 (Figure 1). As shown in Figure 5, trypsin cleavage of labeled receptors, followed by deglycosylation, produced labeled fragments of 8 kDa in both mouse and human receptors, while an additional 3.5 kDa fragment was present in the mouse receptor but not in the human receptor. In the absence of deglycosylation, the 8 and 3.5 kDa fragments migrated as broad bands with much larger MW_{app}, indicating that they contain one or both of the glycosylation sites (N4 and N18). The same result was obtained when deglycosylation was performed before rather than after trypsin cleavage (not shown). The 8 kDa fragment is consistent with cleavage at the cluster of basic residues in the first intracellular loop of both receptors (Figure 1), while the 3.5 kDa fragment is consistent with cleavage at K27 in the mouse receptor only. This interpretation was confirmed by showing that the 8 kDa fragment was membrane-associated, while the 3.5 kDa fragment remained in the supernatant after centrifugation of the membranes (Figure 6). These results confirm localization of the attachment site between the N-terminus and K27.

Evidence for Disulfide Bridges. The effects of sulfhydryl- and disulfide-reactive reagents on binding of a high affinity radioligand to the GnRH receptor are shown in Figure 7. DTT (25 mM) abolished binding, indicating the existence of at least one disulfide bridge that is important for ligand binding. NEM and iodoacetamide had no effect on binding at concentrations up to 25 mM (Figure 7), indicating that free sulfhydryls are either absent, not necessary for binding, or are buried in the protein and inaccessible to the reagents.

In the photoaffinity labeled receptors cleaved with Glu-C, both the 13 kDa fragment from the mWT receptor and the 8 kDa fragment from the hWT receptor were present, with unchanged mobility, under both reducing and nonreducing conditions (Figures 3 and 8). In contrast, under nonreducing conditions, the 18 kDa fragment derived from the mE90Q receptor was absent, and instead the cleaved receptor migrated with similar mobility to the uncleaved receptor (Figure 8). The C-terminal end of the 18 kDa fragment seen in the mE90Q receptor is most likely to be residue E156 for the following reasons: (i) Its size (18 kDa) is too large to be consistent with cleavage at E111Q, which would generate a fragment of 13 kDa, while cleavage at E156 would yield a fragment of expected size 18 kDa; (ii) In partial digestions of mouse wild-type and E111Q mutant receptors, there were no differences in the pattern of labeled fragments (not shown), indicating that the enzyme does not cleave at

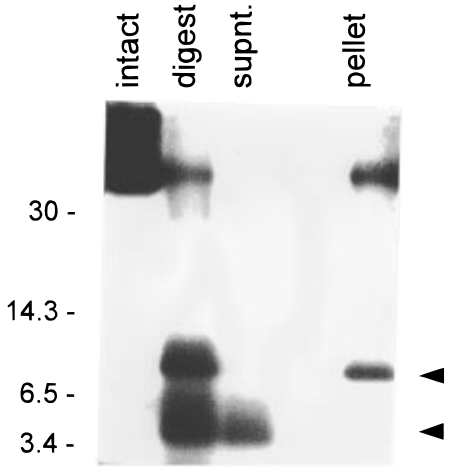

FIGURE 6: Trypsin cleavage of photoaffinity labeled mouse GnRH receptor generates a soluble 3.5 kDa labeled fragment. αT3 cells were photoaffinity labeled, and membranes were deglycosylated as described in Experimental Procedures (intact), following which the membrane suspension was incubated with 200 μg/mL trypsin at 37 °C for 18 h (digest). After centrifugation at 10000*g* for 30 min, the supernatant was removed (supnt.) and the pellet was dissolved in SDS sample buffer (pellet). Arrowheads indicate the 3.5 and 8 kDa fragments referred to in the text.

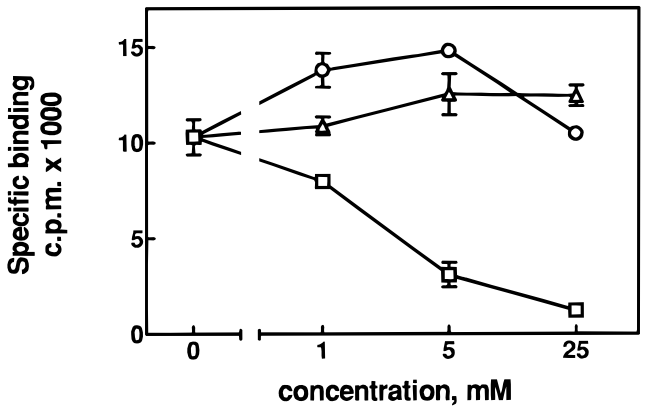

FIGURE 7: Effects of sulfhydryl- and disulfide-reactive compounds on GnRH analog binding. Binding of GnRH analog tracer to membranes from αT3 cells was performed as described in Experimental Procedures, in the presence of the indicated concentrations of dithiothreitol (squares), *N*-ethylmaleimide (triangles), or iodoacetamide (circles).

E111. Thus, the 18 kDa fragment derived from mE90Q includes the first extracellular loop and residue C114. The fact that this fragment was visible only after reduction indicates that a disulfide bridge links C114 to another portion of the receptor, resulting in a large fragment under nonreducing conditions with similar mobility to the uncleaved receptor.

To determine which residue is linked to C114 and to probe the existence of a second disulfide bridge, the effects of mutating C14, C196, and C200 to serine on receptor function were investigated. The hC196S mutant showed no detectable agonist stimulation of inositol phosphate production (Figure 9). The mutants hC14S and hC200S both displayed closely similar phenotypes, comprising a loss of potency and a decrease in maximal GnRH-stimulated inositol phosphate production. hC14S showed a mean 25.9-fold increase in EC_{50} ($n = 4$ experiments) and a mean 36% decrease in maximal inositol phosphate response ($n = 5$), while hC200S showed a mean 16.9-fold increase in EC_{50} ($n = 4$) and a

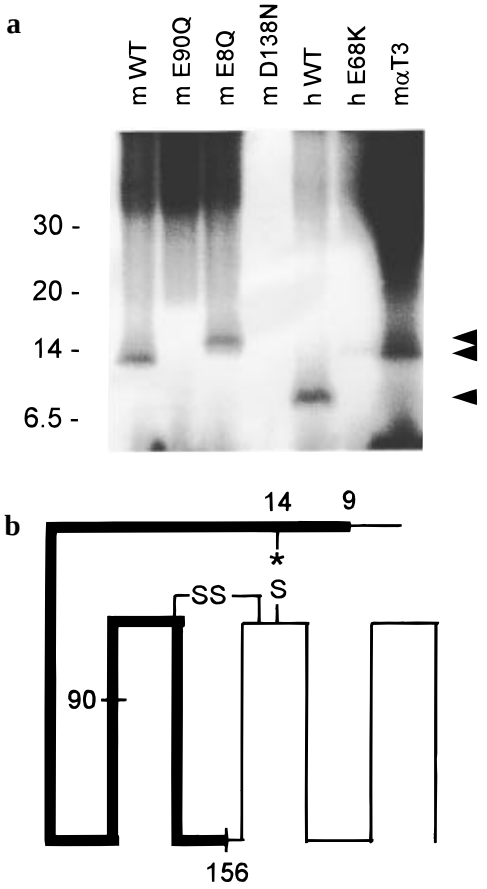

FIGURE 8: Endoproteinase Glu-C cleavage of photoaffinity labeled GnRH receptors: SDS-PAGE under nonreducing conditions. (a) COS-1 cells expressing mouse or human GnRHRs and αT3 cells were photoaffinity labeled; membrane suspensions were solubilized, deglycosylated, and digested with Glu-C under nonreducing conditions as described under Experimental Procedures. After digestion, gel electrophoresis was performed without addition of reducing agent, followed by autoradiography. Arrowheads indicate 8, 13, and 14 kDa labeled fragments referred to in the text. (b) Relationship of labeled Glu-C fragments to disulfide bridges. The heavy line shows the 18 kDa fragment from the E90Q receptor that is released from the rest of the receptor under reducing conditions. The asterisk (*) indicates the attachment site of the radiolabeled peptide.

mean 33% decrease in maximal response ($n = 5$) (Figure 9). The effects of C14S and C200S mutations were nonadditive in the double mutant hC14S/C200S, which showed a mean 25.0-fold loss of potency for GnRH ($n = 2$), similar to the single mutants. Surprisingly, the maximal inositol phosphate response was restored to normal in the double mutant (Figure 9). The levels of radioligand binding in all the cysteine mutants were too low to allow estimates of affinity and receptor number (data not shown), probably due to a combination of low affinity and low expression.

DISCUSSION

In this study, we utilized mutation of endoproteinase cleavage sites to localize the attachment site of the photoreactive GnRH agonist [D-Lys^6-N-azidobenzoyl]GnRH to a seven-residue segment comprising residues 12−18 of the N-terminal domain of the GnRHR. This method should be generally applicable to low abundance proteins that can be covalently labeled without the need for purification.

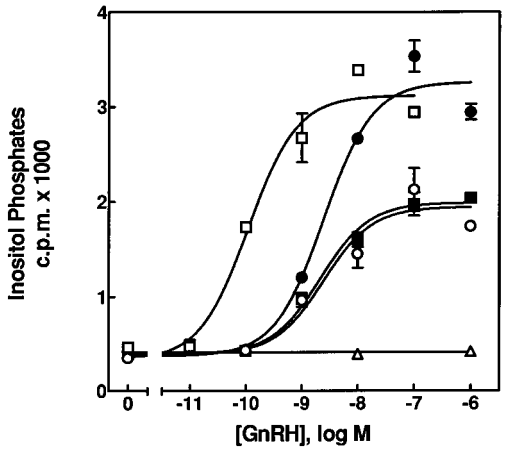

FIGURE 9: GnRH-stimulated inositol phosphate production by human wild-type and Cys mutant receptors. Open squares, hWT receptor; open circles, hC14S mutant; filled squares, hC200S mutant; filled circles, hC14S/C200S double mutant; triangles, hC196S mutant.

Localization of the attachment site provided a direct test of the existence of a putative disulfide bridge between the first and second extracellular loops of the GnRHR. A disulfide bridge in this position is believed to be present in the majority of GPCRs because of the high degree of conservation within the GPCR superfamily of the Cys residue at the C-terminal end of the first extracellular loop (C114 in the GnRHR) and a second Cys somewhere in the second extracellular loop. Evidence for the existence of this bridge has come from several experimental approaches. In rhodopsin, its existence has been conclusively demonstrated by reactivity of the free sulfhydryl groups following prior reduction and identification of the reactive groups by protein sequencing or site-directed mutagenesis (*28*, *29*). In the β-adrenergic receptor, mutation of these Cys residues to valines caused complex effects on agonist binding, which were nonadditive in the double mutant, suggesting the existence of a disulfide bridge (*30*). In the angiotensin II type 1A receptor, analysis of single and double Cys to Gly mutations indicated the presence of both the conserved disulfide bridge and a second bridge linking the N-terminal domain to the third extracellular loop (*31*). Finally, ligand cross-linking combined with cleavage and analysis of labeled fragments by gel electrophoresis directly confirmed the existence of the conserved disulfide bridge in the muscarinic (*32*) and substance P receptors (*33*).

In the present study, we show that, in the GnRHR, C114 is disulfide-bonded to one of the Cys residues in the second extracellular loop. The evidence for this is that the 18 kDa labeled fragment of the mE90Q receptor, which includes residue C114, was shown to be free under reducing conditions but linked to another segment of the receptor under nonreducing conditions. Mutation of the Cys residues was used to distinguish whether C114 was linked to C196 or C200. Mutation of either C14 or C200 to serine produced similar phenotypes, comprising a loss of potency and a decrease in maximal inositol phosphate response, and these effects were nonadditive in the C14S/C200S double mutant, suggesting that C14 and C200 are disulfide-linked. In contrast, mutation of C196 to serine resulted in a severe disruption of function, with complete loss of inositol phosphate response and no measurable binding, consistent with its involvement with C114 in the highly conserved disulfide bridge. Taken together, the results indicate that, in the human GnRH receptor, disulfide bridges exist between the residues C14−C200 and C114−C196.

The converse possibility, i.e., that C14 and either C196 or C200 are involved in ligand binding as free sulfhydryls, is not supported by the results, as in that case the double Cys mutation would be expected to show a more severe impairment of function than the single mutants. In addition, the lack of effects of NEM and iodoacetamide on ligand binding suggest that free sulfhydryl groups are not present, are not involved in binding, or are inaccessible to the reagents.

The rightward shifts in the dose−response curves for inositol phosphate production in the C14S, C200S, and C14S/C200S mutants are most likely due to a combination of low agonist binding affinity and low expression, resulting from an altered conformation of the N-terminal segment and second extracellular loop in the absence of the C14−C200 disulfide bridge. This is consistent with the very low agonist binding we found. Interestingly, the double Cys mutant displayed a higher maximal inositol phosphate response than the single Cys mutants (Figure 9). A possible explanation for this finding is that, in the single Cys mutants, inappropriate disulfide bridge formation occurs in a proportion of the expressed receptor molecules (i.e., in hC14S, a C114−C200 bridge, and in hC200S a C14−C196 bridge).

In view of the existence of the C14−C200 bridge, as suggested by the mutagenesis results, it is interesting that the 13 kDa Glu-C fragment from the mWT receptor (residues 9−90) and the 8 kDa fragment from the hWT receptor (residues 9−68) were present, with unchanged mobility, under both reducing and nonreducing conditions (Figure 8). Therefore, after photoaffinity cross-linking, the N-terminal domain is no longer disulfide-linked to another segment of the receptor, a finding which implies that the C14/C200 disulfide bond is cleaved in the course of the photolysis reaction.

On theoretical grounds, cleavage of disulfide bridges is expected to be the most favorable reaction of the nitrene free radical generated during photolysis of aryl azido compounds (*34*). In a review of cross-linking experiments, Cys was the second most frequently labeled amino acid residue (after Tyr) (*34*), and in at least one case two adjacent Cys residues involved in a disulfide bond were labeled (*35*). Taken together with these considerations, the present mutagenesis and cross-linking results indicate that the C14−C200 disulfide bridge of the GnRHR is cleaved during the photolysis reaction and suggest C14 as the cross-linked residue. In view of this, we considered the possiblilty that C200 might also be a site of cross-linking; however, the pattern of labeled fragments showed that little or no reaction with C200 takes place.

In the present study, we used a photoreactive GnRH analog with arylazido group attached to residue 6 of the peptide. This residue is unlikely to be involved directly in ordinary ligand binding, since widely differing substitutions at position 6 in GnRH analogs are tolerated without loss of high affinity binding (*36*). The N- and C-terminal residues of GnRH have been highly conserved in evolution (*37*), and receptor binding and activation are very sensitive to substitutions in these regions of the peptide (*36*). Computational modeling of GnRH suggests that the peptide adopts a bent conformation in solution, with the N- and C-termini close together in space

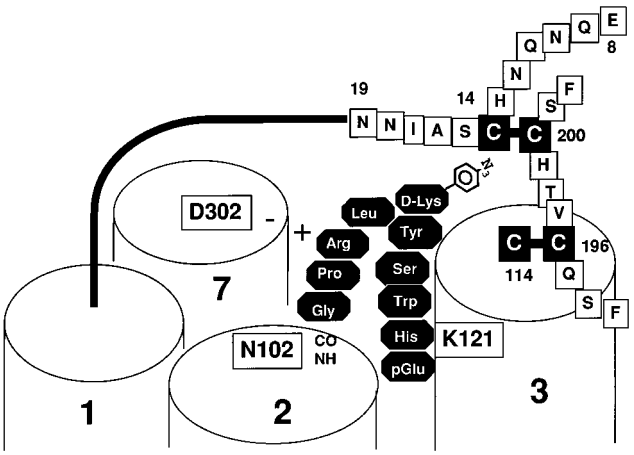

FIGURE 10: Schematic representation of putative GnRH binding site. Numbered cylinders represent the transmembrane helices. The solid curved *line* represents the portion of the N-terminal domain linking the N-terminus to the first transmembrane helix. Cys residues C14−C200 and C114−C196 are shown linked by disulfide bridges. The photoreactive GnRH agonist is shown in its proposed binding site, defined by residues N102, K121, and D302, as described in the text. The benzoylazido group of the photoreactive peptide is shown positioned near to the C14−C200 disulfide bridge, which is cleaved during photolysis.

(*38*−*40*), and this is supported by the fact that the N- and C-termini of GnRH can be recognized as a single epitope by antibodies (*37*). For these reasons, it is believed that the N- and C-termini of the peptide interact with the receptor, while the residue at position 6 probably points away from the binding site.

Current evidence indicates that the binding sites of GPCRs for peptide ligands involve the extracellular domains as well as the interhelical pocket of the receptors (*41*, *42*). In the GnRHR, mutational analysis has provided some insights into the location of the ligand-binding pocket. In the mouse GnRHR, mutation of E301 (D302 in the human GnRHR) to a neutral residue resulted in a loss of selectivity for GnRH analogs with Arg at position 8 of the peptide, suggesting that E301 interacts electrostatically with Arg8 of GnRH (*17*). In the human GnRH receptor, the N102 side chain has been shown to play a role in binding of the C-terminus of the peptide, possibly by H-bonding with the C-terminal glycinamide moiety (*43*). Finally, mutation of K121 of the human GnRHR resulted in a loss of agonist affinity, while high affinity for an antagonist was retained, suggesting that the N-terminus of GnRH, which is required for agonist activity, may interact with K121 (*44*). These ligand−receptor interactions are based purely on mutational evidence and should be regarded as working hypotheses rather than definitive assignments. Nevertheless, they are represented schematically in Figure 10 together with the two disulfide bridges demonstrated in the present study and the proposed interaction between the arylazido group and the C14−C200 bridge. It is evident that the ligand-binding pocket defined by current evidence is located at the level of the extracellular ends of the transmembrane helices, with the N-terminus of GnRH extending deeper into the transmembrane helix bundle. The sides of the pocket are bounded by the first and third extracellular loops, while the N-terminal domain, tethered to the second extracellular loop, forms its roof.

The fact that the GnRH receptor remained irreversibly activated following cross-linking with [azidobenzoyl-D-Lys^6]-GnRH indicates that the tethered agonist peptide remained docked in its correct orientation in the binding site. This validates the use of the cross-link site on the N-terminal segment of the receptor as a constraint on computational models of the GnRH binding site. Further studies using other photoreactive GnRH analogs with photoreactive groups in different positions on the peptide are needed to provide more direct information regarding the location of ligand−receptor contact sites.

In summary, we have shown that a photoreactive GnRH agonist analog cross-links to a seven-residue segment comprising residues 12−18 of the N-terminal domain of the human GnRH receptor. This localization permits direct demonstration of a disulfide bridge (C114−C196) between the first and second extracellular loops. Analysis of the functional effects of mutation of the Cys residues indicates that a second disulfide bridge (C14−C200) links the N-terminal domain with the second extracellular loop.

ACKNOWLEDGMENT

We thank David McIntosh for his invaluable contribution in development of the photoaffinity labeling protocols and P. Mellon for the gift of αT3 cells. Supported by the South African Medical Research Council, the Foundation for Research and Development, and the University of Cape Town.

REFERENCES

1. Tsutsumi, M., Zhou, W., Millar, R. P., Mellon, P. L., Roberts, J. L., Flanagan, C. A., Dong, K., Gillo, B., and Sealfon, S. C. (1992) *Mol. Endocrinol. 6*, 1163−1169.
2. Kakar, S. S., Musgrove, L. C., Devor, D. C., Sellers, J. C., Neill, J. D. (1992) *Biochem. Biophys. Res. Commun. 189*, 289−295.
3. Kaiser, U. B., Zhao, D., Cardona, G. R. and Chin, W. W. (1992) *Biochem. Biophys. Res. Comm. 189*, 1645−1652.
4. Reinhart, J., Mertz, L. M., and Catt, K. J. (1992) *J. Biol. Chem. 267*, 21281−21284.
5. Chi, L., Zhou, W., Prikhozhan, A., Flanagan, C., Davidson, J. S., Golembo, M., Illing, N., Millar, R. P., and Sealfon, S. C. (1993) *Mol. Cell. Endocrinol. 91*, R1−R6.
6. Illing, N., Jacobs, G. F. M., Becker, I. I., Flanagan, C., Davidson, J. S., and Millar, R. P. (1993) *Biochem. Biophys. Res. Commun. 196*, 745−751.
7. Kakar, S. S., Rahe, C. H., and Neill, J. D. (1993) *Domest. Anim. Endocrinol. 10*, 335−342.
8. Tse, A., and Hille, B. (1992) *Science 255*, 462−464.
9. Stojilkovic, S. S., and Catt, K. J. (1992) *Endocr. Rev. 13*, 256−280.
10. McArdle, C. A., Bunting, R., and Mason, W. T. (1992) *Mol. Cell. Neurosci. 3*, 124−132.
11. van der Merwe, P. A., Millar, R. P., Wakefield, I. K., and Davidson, J. S. (1989) *Biochem. J. 264*, 901−908.
12. Davidson, J. S., van der Merwe, P. A., Wakefield, I. K., and Millar, R. P. (1991) *Mol. Cell. Endocrinol. 76*, C33−C38.
13. Tse, A., and Hille, B. (1993) *Science 260*, 82−84.
14. Probst, W. C., Snyder, L. A., Schuster, D. I., Brosius, J., and Sealfon, S. C. (1992) *DNA Cell Biol. 11*, 1−20.
15. Brown, E. M., Gamba, G., Riccardi, D., Lombardi, M., Butters, R., Kifor, O., Sun, A., Hediger, M. A., Lytton, J., and Hebert, S. C. (1993) *Nature 366*, 575−580.
16. Juppner, H., Abou-Samra, A. B., Freeman, M., Kong, X. F., Schipani, E., Richards, J., Kolakowski, L. F., Jr., Hock, J., Potts, J. T., Jr., and Kronenberg, H. M. (1991) *Science 254*, 1024−1026.
17. Flanagan, C. A., Becker, I. I., Davidson, J. S., Wakefield, I. K., Zhou, W., Sealfon, S. C., and Millar, R. P. (1994) *J. Biol. Chem. 269*, 22636−22641.

18. Kunkel, T. A., Bebenek, K., and McClary, J. (1987) *Methods Enzymol. 204*, 125−139.
19. Keown, W. A., Campbell, C. R., and Kucherlapati, R. S. (1990) *Methods Enzymol. 185*, 527−537.
20. Hazum, E. (1981) *Endocrinology 109*, 1281−1283.
21. Windle, J. J., Weiner, R. I., and Mellon, P. L. (1990) *Mol. Endocrinol. 4*, 597−603.
22. Schagger, H., and von Jagow, G. (1987) *Anal. Biochem. 166*, 368−379.
23. Davidson, J. S., Wakefield, I. K., Sohnius, U., van der Merwe, P. A., and Millar, R. P. (1990) *Endocrinology 126*, 80−87.
24. Janovick, J. A., Haviv, F., Fitzpatrick, T. D., and Conn, P. M. (1993) *Endocrinology 133*, 942−945.
25. Perrin, M. H., Bilezikjian, L. M., Hoegner, C., Donaldson, C. J., Rivier, J., Haas, Y., and Vale, W. (1993) *Biochem. Biophys. Res. Commun. 191*, 1139−1144.
26. Davidson, J. S., Flanagan, C. A., Zhou, W., Becker, I. I., Elario, R., Emeran, W., Sealfon, S. C., and Millar, R. P. (1995) *Mol. Cell. Endocrinol. 107*, 241−245.
27. Houmard, J., and Drapeau, G. R. (1972) *Proc. Natl. Acad. Sci. U.S.A. 69*, 3506−3510.
28. Al-Saleh, S., Gore, M., and Akhtar, M. (1987) *Biochem. J. 246*, 131−137.
29. Karnik, S. S., and Khorana, H. G. (1990) *J. Biol. Chem 265*, 17520−17524.
30. Dixon, R. A. F., Sigal, I. S., Candelore, M. R., Register, R. B., Scattergood, W., Rands, E., and Strader, C. D. (1987). *EMBO J. 6*, 3269−3275.
31. Ohyama, K., Yamano, Y., Sano, T., Nakagomi, Y., Hamakubo, T., Morishima, I., and Inagami, T. (1995). *Regul. Pept. 57*, 141−147.
32. Curtis, C. A. M., Wheatley, M., Bansal, S., Birdsall, N. J. M., Eveleigh, P., Pedder, E. K., Poyner, D., and Hulme, E. C. (1989) *J. Biol. Chem. 264*, 489−495.
33. Boyd, N. D., Kage, R., Dumas, J. J., Krause, J. E., and Leeman, S. E. (1996) *Proc. Natl. Acad. Sci. U.S.A. 93*, 433−437.
34. Kotzyba-Hibert, F., Kapfer, I., and Goeldner, M. (1995) *Angew. Chem. Int. Ed. Engl. 34*, 1296−1312.
35. Dennis, M., Giraudat, J., Kotzyba-Hibert, F., Goeldner, M., Hirth, C., Chang, J. Y., Lazure, C., Chretien, M., and Changeux, J. P. (1988) *Biochemistry 27*, 2346−2357.
36. Karten, M. J., and Rivier, J. E. (1986) *Endocr. Rev. 7*, 44−66.
37. King, J. A., and Millar, R. P. (1995) *Cell. Mol. Neurobiol. 15*, 5−23.
38. Monahan, M. W., Amoss, M. S., Anderson, H. A., and Vale, W. (1973) *Biochemistry 12*, 4616−4621.
39. Momany, F. A. (1976) *J. Am. Chem. Soc. 98*, 2990−2995.
40. Freidinger, R. M., Veber, D. F., Perlow, D. S., Brooks, J. R., and Saperstein, R. (1980) *Science 210*, 656−658.
41. Strader, C. D., Fong, T. M., Tota, M. R., Underwood, D., and Dixon, R. A. (1994) *Annu. Rev. Biochem. 63*, 101−132.
42. Schwartz, T. W. (1994) *Curr. Opin. Biotechnol. 5*, 434−444.
43. Davidson, J. S., McArdle, C. A., Davies, P., Elario, R., Flanagan, C., and Millar, R. P. (1996) *J. Biol. Chem. 271*, 15510−15514.
44. Zhou, W., Rodic, V., Kitanovic, S., Flanagan, C. A., Chi, L., Weinstein, H., Maayani, S., Millar, R. P., and Sealfon, S. C. (1995) *J. Biol. Chem. 270*, 18853−18857.

BI971377T